Lab on a Chip

PAPER

View Article Online
View Journal | View Issue

Cite this: *Lab Chip*, 2020, **20**, 626

Intelligent optofluidic analysis for ultrafast single bacterium profiling of cellulose production and morphology†

Jiaqing Yu,[a] Guoyun Sun,[a] Nicholas Weikang Lin,[a] Sundaravadanam Vishnu Vadanan,[b] Sierin Lim [b] and Chia-Hung Chen *[c]

Received 8th November 2019,
Accepted 29th December 2019

DOI: 10.1039/c9lc01105f

rsc.li/loc

Bacterial cellulose (BC), a renewable type of cellulose, has been used in the manufacture of foods, cosmetics, and biomedical products. To produce BC, a high-throughput single-bacterium measurement is necessary to identify the functional bacteria that can produce BC with sufficient amount and desirable morphology. In this study, a continuous-flow intelligent optofluidic device was developed to enable high-throughput single-bacterium profiling of BC. Single bacteria were incubated in agarose hydrogel particles to produce BC with varied densities and structures. An intelligent convolutional neural network (CNN) computational method was developed to analyze the scattering patterns of BC. The BC production and morphology were determined with a throughput of ~35 bacteria per second. A total of ~10^5 single-bacterium BC samples were characterized within 3 hours. The high flexibility of this approach facilitates high-throughput comprehensive single-cell production analysis for a range of applications in engineering biology.

Introduction

Compared to conventional cellulose isolated from wood pulp, bacterial cellulose (BC) has high purity (due to the absence of lignin and hemicellulose) and good physical properties. Based on the morphology of BC, promising applications in the fabrication of wound dressings, drug carriers, foods, cosmetics and artificial vessels have been demonstrated.[1,2] However, the efficiency of current BC production methods is relatively low, limiting the industrial value of BC due to the lack of a high-throughput measurement platform for the statistical analysis of BC production by individual bacteria in a mutant library. Moreover, the ability of current analytical approaches to effectively determine BC structure and morphology produced by single bacteria is limited. Despite various attempts to modify the biosynthetic pathway, the measurement of modified bacteria to fabricate desired cellulose products requires weeks to months with limited measurement parameters.[3,4]

At present, two broad categories of methods are available for single-bacterium analysis: flow cytometry and microwell-based platforms. A promising tool for single-cell screening with a throughput of ~10^4 cells per min, flow cytometry is widely used to measure cell size, surface biomarkers and intracellular signal molecules.[5–8] Through fluorescence labeling of cell-encapsulated hydrogel particles, cellular antibody secretion is measured.[5] The droplet-based hydrogel technology is designed to encapsulate bacteria to determine their proliferation using flow cytometry.[6] The flow cytometry-based approach has been extended to integrate drop-screen technology for synthetic biology applications.[9] Although the above applications have been demonstrated, determining the secretion amount and morphology of products such as BC remains a challenge. Moreover, most flow cytometry platforms are dependent on fluorescence readouts, and the fluorescence labeling process affects cell viability after screening.

The microwell-based platform has been developed to measure single-bacterium biological products, such as BC, after long-term culture[10–13] and was designed specifically for function-driven single-cell screen.[12,13] For example, cellulose degradation is evaluated to identify cellulose-degrading bacteria from the rare biosphere.[14] However, the screening throughput of microwell-based approaches is limited by the number of microwells in one microtiter plate (~100–1000 per experimental run). Moreover, capturing a single cell/bacterium in each microwell with high efficiency remains

[a] *Department of Biomedical Engineering, National University of Singapore, 117575 Singapore*
[b] *School of Chemical and Biomedical Engineering, Nanyang Technological University, 637457 Singapore*
[c] *Department of Biomedical Engineering, City University of Hong Kong, 83 Tat Chee Avenue, Kowloon Tong, Hong Kong. E-mail: chiachen@cityu.edu.hk*
† Electronic supplementary information (ESI) available. See DOI: 10.1039/c9lc01105f

challenging. Our previous study reported the use of a swim plate as a platform, which allowed the evaluation of environmental impacts on BC production, but the throughput was still limited.[15]

Droplet microfluidics has emerged as an important platform that provides new experimental possibilities for high-throughput screening.[16,17] The continuous generation of large amounts of monodispersed droplets containing a single cell or bacterium (1 kHz to 10 kHz generation rates) enables effective compartmentalization for molecule secretion analysis.[18,19] For example, cell-secreted enzyme activities have been investigated by inserting fluorescence resonance energy transfer (FRET)-based sensors within droplets for high-throughput biological sample profiling.[20–22] Many organisms (such as *C. elegans*) could be encapsulated for rapid characterization.[23] However, the challenge of measuring single bacterium bioproduction structures, such as BC morphology, remains. In fact, upon encapsulation, a single bacterium in a droplet requires incubation within the droplet (volume ~1–10 pL) for 3–7 days to allow cell proliferation and BC production. The limited nutrient supply within the droplet might lead to misleading BC measurement outcomes. Several studies using hydrogel particles have been carried out to analyze single cell secretions.[5] For example, bacteria were incubated in hydrogel particles to evaluate cell proliferation by measuring fluorescence signals.[6] However, it was not easy to analyze product structures using the fluorescence labeling approach. Moreover, fluorescence readout requires a labeling process, which might affect cell activities after the measurements.[7,9]

In this study, we developed a label-free intelligent continuous-flow single-bacterium measurement platform to determine BC production and morphology *via* light scattering patterns with a throughput of ~35 bacteria per second. The workflow is presented in Fig. 1. A single bacterium was compartmentalized in agarose hydrogel particles to be cultured for BC production.[24,25] Specifically, the single bacterium was encapsulated in water-in-oil droplets with agarose monomers. The agarose monomers were polymerized to form agarose hydrogel particles. The bacterium-containing hydrogel particles were subsequently incubated under shaking for bacterial proliferation and then maintained under static conditions for cellulose production. To screen the BC produced by a single bacterium in the hydrogel particles, the particles were reinjected into a microfluidic chip for scattering imaging analysis. At the measurement point, laser light was focused on a single BC particle, showing a scattering pattern, and the scattering images were recorded to reflect the BC production and morphology. To rapidly analyze BC using a computational method, convolutional neural networks (CNNs), the BC was classified into one of five categories based on its production amount and morphology. Continuous-flow measurement was performed with a throughput of ~35 bacteria per second. The platforms for measuring BC production were compared and are summarized in ESI† 1 (Table S1). The integration of hydrogel particle encapsulation and data-driven scattering image recognition was synergistic. The hydrogel particle approach was used for single-bacterium isolation for BC production, while scattering image analysis *via* CNN allowed high-throughput BC production and morphology profiling.

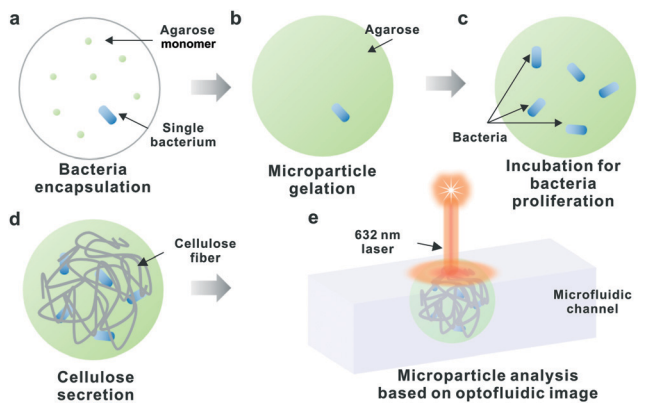

Fig. 1 Schematic of the high-throughput analysis system for BC particles based on scattering imaging with the following steps: (a) encapsulation of a single bacterium in a droplet containing agarose monomers; (b) gelation of agarose; (c) bacterial proliferation inside the agarose particles; (d) BC production by the encapsulated bacterium inside the agarose hydrogel particle; and (e) capture of scattering images for high-throughput analysis.

Materials and methods

Device fabrication

The device was fabricated according to a standard polydimethylsiloxane (PDMS, Sylgard 184, Dow Corning Inc., Midland, MI) microchannel fabrication method. SU8 photoresist (SU8-2050, MicroChem Inc., Newton, MA) was patterned on a silicon wafer to build a positive master. The positive master mold for the device contained channels that were 30 μm tall. The SU-8 master was treated with trichloro(1*H*,1*H*,2*H*,2*H*-perfluorooctyl)silane (Sigma-Aldrich, St. Louis, MO) for 1 hour to prevent adhesion of the SU-8 features on the master mold to PDMS after molding. The trichloro(1*H*,1*H*,2*H*,2*H*-perfluorooctyl)silane solution was evaporated and deposited on the master in a desiccator with an ~5 psi vacuum.

In the second step, PDMS was degassed for 1 hour in a desiccator with an ~5 psi vacuum and poured onto the master mold. The mold was cured in an oven at 65 °C for 6 hours, and then the PDMS layer was peeled off from the silicon master. Holes were punched through the end of the channels using a Harris Uni-Core puncher with a diameter of 1.00 mm (Ted Pella, USA). To form a hydrophobic surface for making the droplet generator, a glass slide was coated with a layer of PDMS. To obtain a thin coating, PDMS was diluted by adding hexane (Sigma, 1:1 mix) and coated on a glass slide using a spin coater at 1800 rpm. The coated glass was then placed in an oven at 65 °C overnight. After plasma bonding, the device was placed in an oven at 65 °C for more

than 20 hours to form strongly bonded and completely hydrophobic surfaces.

Droplet based bacterial encapsulation

Three cellulose-producing strains were purchased from ATCC: *Gluconacetobacter xylinus* (ATCC® 700178™, USA), *Gluconacetobacter hansenii* (ATCC® 53582™, USA), and *Komagataeibacter rhaeticus* (ATCC® BAA-2831™ iGEM, USA). The 459 YGC culture medium consisted of 50.0 g of glucose, 5.0 g of yeast extract, 12.5 g of $CaCO_3$ and 15.0 g of agar in 1.0 L of distilled water. The medium was autoclaved at 121 °C for 15 min. The density-matching agent Percoll (Sigma P4937) was added (25% v/v) into the solution. The bacteria concentration was 5×10^7 bacteria per mL. To prepare agarose hydrogel particles, agarose (Sigma A2576) powder was dissolved in bacterial culture medium to make a 1.5% (w/v) agarose monomer solution. HFE-7500 fluorocarbon oil (3M Novec) with 2% surfactant (Krytox modified with polyethylene glycol) was used as the oil phase. A PDMS device with a short-pinched flow channel and a cross-junction droplet generator (30 μm in depth and 30 μm in width) was fabricated to generate agarose droplets for single-bacterium encapsulation.[21] The hydrophobic wettability of PDMS allows the formation of monodispersed water-in-oil agarose droplets. The flowrate of the oil phase used was 5 μL min^{-1}, whereas the flow rate of the bacteria–agarose solution used was 0.5 μL min^{-1} to produce agarose droplets with a diameter of ~30 μm (volume ~10 pL). Based on the Poisson distribution, the single-bacterium encapsulation rate was ~35%. The agarose droplets were generated at 37 °C, collected and then cooled at room temperature (~23 °C) for ~5 hours for agarose gelation. Afterwards, the oil phase was removed by washing with a biocompatible demulsifier, 1*H*,1*H*,2*H*,2*H*-perfluoro-1-octanol (Sigma, 370533). The hydrogel particles containing bacteria were collected and rinsed twice with bacterial culture medium to remove the demulsifier.

Cellulose production

The bacteria in agarose particles were incubated at 37 °C under shaking conditions (150 rpm) for 36 hours for cell proliferation. Afterwards, the bacteria were cultured at room temperature (~23 °C) in static conditions for BC production. The number and viability of the bacteria were verified using SYTO 9 green fluorescent nucleic acid stain (Invitrogen S-34854), as shown in ESI† 2 (Fig. S1). The agarose hydrogel particles were incubated with SYTO 9 for 15 min and then washed with culture medium to remove the excess dye. The dye penetrated the porous agarose structure to stain the encapsulated bacteria. SYTO 9 fluorescence was recorded using a Nikon Ti-Eclipse fluorescence microscope with a CoolLED automated excitation light source. The agarose hydrogel particles containing proliferating bacteria were stored at 25 °C in a sealed tube for static incubation, and the bacteria produced a significant amount of cellulose for protection and nourishment. All the cellulose produced by the bacteria remained in the agarose hydrogel particles. The amount, density, and clustering of the cellulose in the hydrogel particles were then analyzed. Fluorescent Brightener 28 (Sigma F3543) solution (10^{-6} mol) was used to stain the cellulose to correlate the results from the scattering to the actual cellulose molecules. The fluorescence signal was observed using an excitation wavelength of 378 nm (and an emission wavelength of 435 nm). Scanning electron microscopy (SEM) images of the cellulose fibers were recorded using an FEI Quanta 200 scanning electron microscope.

High throughput scattering analysis

After incubation, the agarose hydrogel particles containing bacteria and BC were collected, washed and suspended in PBS. Polyvinyl alcohol (Sigma 341 584) was placed on the microfluidic channel with a hydrophilic surface to reinject the hydrogel particle suspension into the microfluidic device. A laser (λ = 632.8 nm, 800 mW, Thor Lab, USA) was used as the incident light source. The beam was reflected by a beam splitter and focused on a single hydrogel particle at the measurement point in the device. The optofluidic image of the light scattered from the hydrogel particle was captured at a distance of 8 mm with a highly sensitive CCD camera with 200 fps (Hamamatsu C13440). The flow rate to upload the hydrogel particles to the measurement platform was 10 μL min^{-1}. Accordingly, the measurement throughput was ~100 particles per second (~35 bacteria per second, with a single-bacterium encapsulation rate of ~35%). A raw video is included in ESI† Video S1. For the hydrogel particles without any inclusion, the scattering image showed the Fraunhofer diffraction pattern of a sphere. However, for particles containing BC, the scattering image showed a deformed fringe pattern decorated by random speckles, resulting from light being reflected and refracted by the inclusions. The captured scattering image was then uploaded to a computer for analysis by CNN. Using the MATLAB-based CNN toolbox, the CNN was trained on the captured imaging data of BC with different morphologies. The pretrained model could perform transfer learning to automatically recognize and classify the new input imaging data of unknown BC hydrogel particles. The analysis result output was indicated as the class scores.

Results and discussion

Bacterial encapsulation, proliferation and cellulose production

Fig. 2 shows micrographs of the BC agarose hydrogel particles resulting from bacterial encapsulation and BC production. First, water-in-oil droplets containing agarose monomers and encapsulating a single bacterium were generated using a droplet generator at 37 °C. (Fig. 2a). Second, the agarose droplets were polymerized by cooling at room temperature (23 °C) to form the agarose hydrogel

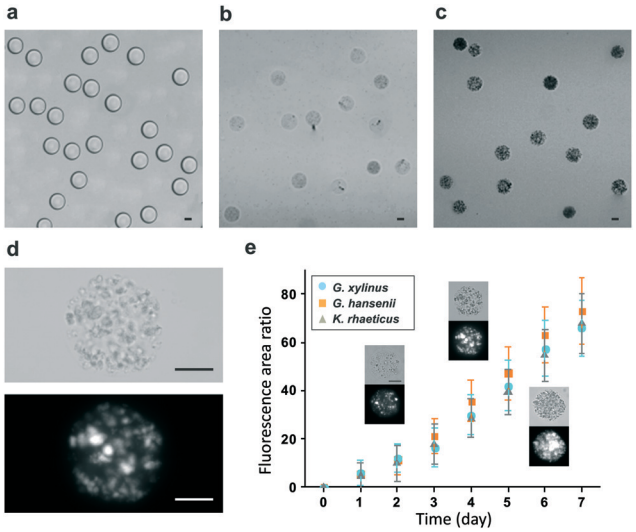

Fig. 2 Single-bacterium (*G. xylinus*) encapsulation and cellulose production inside agarose hydrogel particles. (a) Droplets containing a single bacterium and agarose monomers. (b) Agarose hydrogel particles containing a single bacterium immersed in culture medium. (c) Agarose hydrogel particles containing secreted BC fibers after 7 days of static incubation. (d) Brightfield and fluorescence microscopy images of BC inside a hydrogel particle obtained by staining with Fluorescent Brightener 28. (e) Increase in cellulose production inside hydrogel particles as indicated by fluorescence staining. Scale bar: 15 μm.

particles. These hydrogel particles were washed by using a biocompatible demulsifier and resuspended in bacterial culture medium (Fig. 2b). The bacteria were incubated at 37 °C under shaking conditions for bacterial proliferation. Afterwards, they were cultured at room temperature (~23 °C) under static conditions for BC production. The produced BC fibers became entangled in the agarose and finally generated BC-containing agarose hydrogel particles (Fig. 2c). The morphology of the cellulose produced in one hydrogel particle was observed by brightfield microscopy (Fig. 2d, upper image). The fluorescence image of BC stained with Fluorescent Brightener 28 is shown in Fig. 2d (lower image). The BC fibers produced by bacteria cultured in agarose hydrogel particles are shown in Fig. 2e. It should be noted that the size of the BC fibrils is consistent with our previous studies, suggesting that the fibrils were grown into the pores of the agarose hydrogel particles.[2] The cellulose production, which was quantified from the fluorescent area stained by Fluorescent Brightener 28, is shown in Fig. 2f. Within the hydrogel particles, BC was produced consistently, resulting in an increase in fluorescence intensity over time. The brightfield and fluorescence microscopy images inside the graph indicate the BC production process on days 3, 5, and 7.

Categorization of the BC

To achieve a high-throughput, label-free imaging analysis system for BC produced by bacteria captured in agarose hydrogel particles, the correlation between the scattering pattern and BC morphology was determined. The brightfield images were taken using a previously developed optical system.[26] Two cameras were used simultaneously to record brightfield images and scattering images. After the correlation was determined, the scattering image, which was captured at relatively low resolution and high speed, was analyzed using (CNN) computation, a type of deep, feed-forward artificial neural network. CNN has been successfully applied to learn and analyze image data without the need for manual feature extraction.

To perform CNN, five categories were defined based on the amount and morphology of the BC: I. small amount of BC; II. medium amount of BC speckle fibers; III. large amount of BC speckle fibers; IV. medium amount of BC agglomerates; and V. large amount of BC agglomerates. Fig. 3 shows schematic drawings and representative photos of the scattering images and brightfield images of single particles. The five categories were manually labeled. A total of 2500 images were recorded. Five hundred paired images (brightfield images and corresponding light scattering images) were recorded for each category to construct a database. It is worth noting that BC with different morphologies demonstrates varied features for specific applications. For example, BC with loose and porous structures (BC speckles, categories II and III) could encapsulate a certain amount of water for applications in fabricating wound dressing membranes and soft scaffolds for tissue regeneration.[14] For example, BC with dense packing aggregations (BC agglomerates, category IV and V) demonstrating robust mechanical strength are suitable for fabricating supporting materials, such as artificial blood vessels.[27] Three known bacterial strains (*G. xylinus, G. hansenii, and K. rhaeticus*) were measured using this platform. The data obtained were consistent with previous results obtained using conventional cell culture methods.[14,27] We demonstrated that these five defined categories could be rapidly identified using our approach, which would be helpful to determine which type of bacteria is suitable for producing BC with the desired amount and morphologies for the desired applications. A summary of BC applications based on the defined morphologies is provided in ESI† 3, Table S2.

CNN computation

To examine the morphology of BC contained in the hydrogel particles *via* scattering patterns, a CNN method was established. The CNN was a classifier with an input of a monochromatic 128 × 128 pixel scattering image and an output of five defined categories. CNN can conduct feature learning of a scattering image through a series of convolutional layers with rectified linear units (ReLU) and pooling processes. A total of 2500 monochromatic 128 × 128 pixel scattering images (500 for each category) with BC morphologies were chosen randomly for algorithm training.

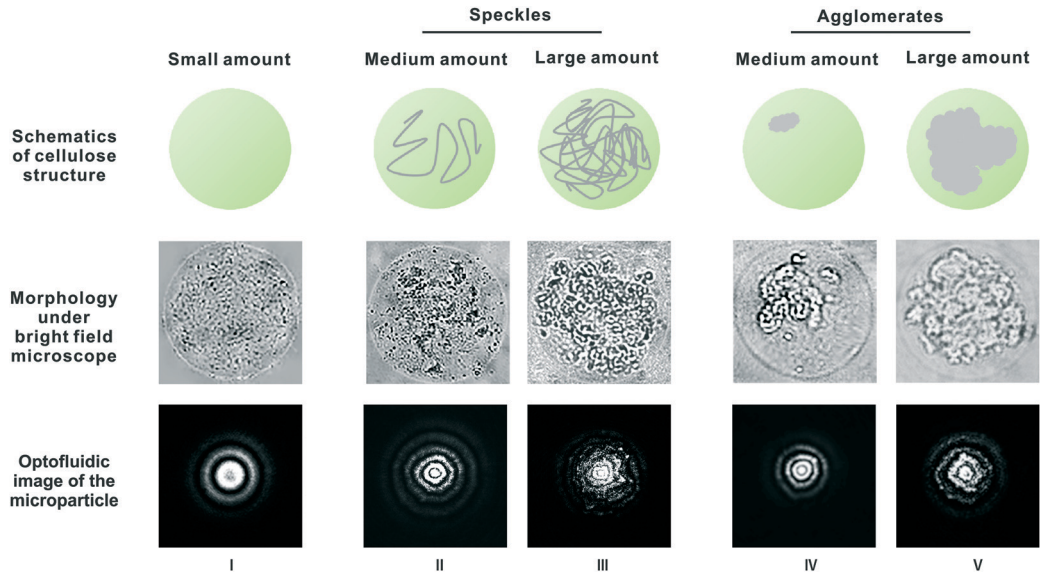

Fig. 3 Five catalogs of BC are identified based on the amount and morphology of the BC: I. small amount of BC; II. medium amount of BC speckles; III. large amount of BC speckles; IV. medium amount of BC agglomerates; and V. large amount of BC agglomerates. The applications of BC are dependent on morphology, which is determined by recording light scattering patterns. For CNN analysis, 2500 images (500 images for each category) were labelled to form a database.

The training process was accomplished when accuracy could not be further improved by the algorithm. The workflow to prepare the CNN database is elaborated in ESI† 4 (Fig. S2). The CNN training process is attached in ESI† 5 (Fig. S3). The program code of CNN used is included in ESI† 6.

Fig. 4 shows the process of capturing an optofluidic scattering image of a BC-containing hydrogel particle flowing in the microfluidic device and the training process of the CNN based on the captured image. Fig. 4a shows the results of classifying the scattering images into the five categories defined in Fig. 3 by running the CNN training processes. An analysis of a single input scattering image is shown on the left side. We input one image from the known category IV into the CNN. The CNN determined the probability that each category best described the input image to be 80% for category IV, 18% for category II and less than 2% for other categories, then defined the image as category IV (Fig. 4b and c). For each category, the CNN analyzed all 500 scattering images, and the analysis accuracy reflected the percentage of images assigned to the correct category. The heat map on the right-hand side indicates the analytical accuracy for the five categories. An accuracy of 100% could not be reached, but increasing the number of images in the database would significantly improve the accuracy. We also merged and rearranged the categories based on a single criterion. We conducted the CNN to analyze the amount of BC production in the particle by analyzing the scattering image, as shown in Fig. 3c. In this example, the result indicated that the particle contained medium amounts of BC, and the accuracy was evaluated by a heat map. Similarly, a single criterion analysis was conducted for BC shape, as shown in Fig. 4d. All of the analyses had excellent accuracy, which means that the CNN training process was completed and that we could use this training network to recognize unknown inputs. The accuracy of our CNN could be improved by including a regression strategy (ESI† 7).

Bacteria cellulose scattering analysis

To investigate the amount and speed of BC secretion at high throughput, three cellulose-secreting species, *G. xylinus*, *G. hansenii*, and *K. rhaeticus*, were selected and encapsulated as single bacterium in the agarose hydrogel particles. The bacteria in the agarose hydrogel particles were incubated under static conditions for different periods (3 days, 5 days and 7 days) and screened by the scattering image-based system to analyze the secreted BC (Fig. 5). The scattering image of a single hydrogel particle was captured, and the measurement throughput reached approximately 100 particles per second. The analysis results indicated that for all three strains, the BC secretion amount increased with time. On day 3, the percentage of hydrogel particles classified as small amount (category I) was relatively high, while on day 7, the proportion of hydrogel particles was classified as large amount (categories III and V). On day 7, the total amount of cellulose secreted by *G. hansenii* was higher than the amount secreted by *K. rhaeticus*, and *G. xylinus* secreted the lowest amount. The percentage of hydrogel particles classified as large amounts (categories III and V) was evaluated. The preference for glucose by *G. hansenii* is consistent with the results of our previous study using a swim plate as a screening platform.[15] Additionally, if we focus on one time point (day 5) for a single strain (*G. hansenii*), hydrogel particles classified as a small amount (category I), medium amount (category IV) and large amount (category V) were discovered simultaneously, showing the heterogeneity of the

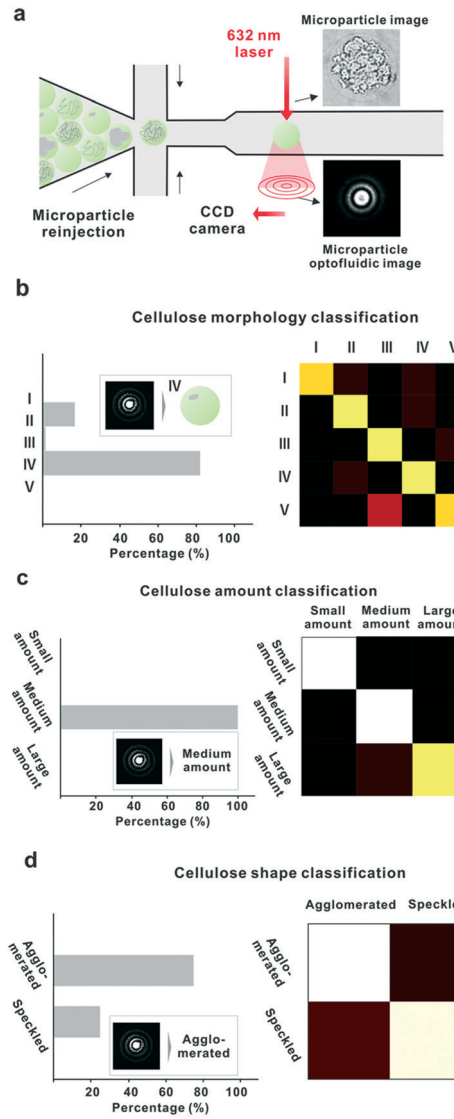

Fig. 4 Process of capturing a scattering image of a BC-containing hydrogel particle flowing in the microfluidic device and training process of the CNN based on the captured image. (a) The agarose particles were flowed through a CCD camera for scattering analysis. The input scattering image of a single hydrogel particle from a known category was analyzed by CNN and classified. The accuracy of the analysis results was calculated. The classifications were based on multiple criteria, including (b) the integral five categories defined in Fig. 3; (c) amount of BC; and (d) shape of BC.

strain. Similarly, heterogeneity occurred in other strains at other time points as well. On the other hand, *G. hansenii* secreted BC mainly with an agglomerated shape, and *K. rhaeticus* tended to secrete speckle-shaped cellulose. *G. xylinus* secreted BC with both shapes, which demonstrated high heterogeneity among individuals. The shape diversity could possibly arise from variations in the thickness of cellulose fibers and the spaces between them.

The amount and morphology of BC produced by different strains varied significantly, and heterogeneity existed among individuals even for strains with identical genome sequences. To characterize BC produced by different strains, the

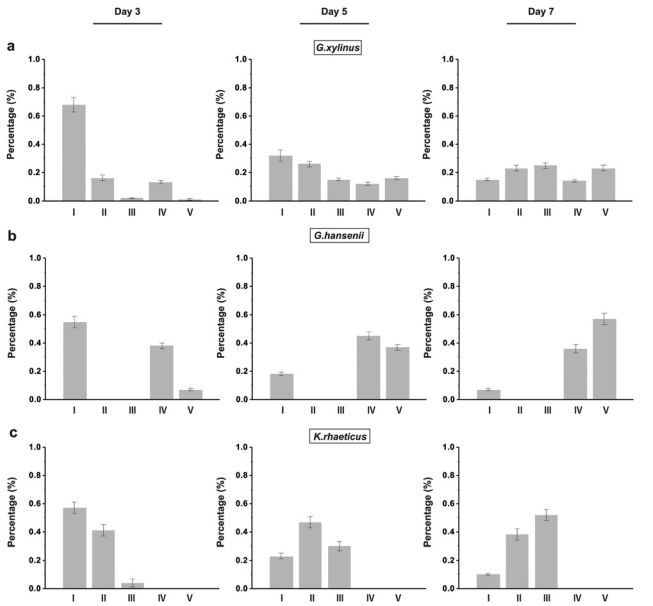

Fig. 5 Classification of a single hydrogel particle based on the scattering images of three different BC-producing species: (a) *Gluconacetobacter xylinus*; (b) *Gluconacetobacter hansenii*; and (c) *Komagataeibacter rhaeticus* after 3, 5 and 7 days of static culture.

nanoscale structural details of their BC were recorded using SEM (ESI† 8, Fig. S4).

Conclusion

BC is an important biosynthesis product for the biomedical industry, and analysis of BC production is desirable for selecting bacterial mutants to fabricate BC with the desired morphology and promising production efficiency. However, challenges remain in high-throughput single-bacterium BC measurement. To address this challenge, several analysis platforms have been investigated though these approaches are labor intensive, and the throughput is relatively limited (~100 to 1000 bacteria per experimental run, which usually takes multiple days to conduct). Continuous-flow measurement technology was previously developed for high-throughput single-cell screening. However, most current techniques are focused on measuring the amount of secretions using a fluorescent staining approach, which has limitations in analyzing product structure (such as BC morphology). Moreover, the labeling process might affect cell activities in subsequent cultures.

In this study, by combining droplet-based hydrogel technology, scattering image analysis and CNN computation, we developed an intelligent platform that enables effective single-bacterium analysis of BC production and morphology with a throughput of ~35 bacteria per second. This platform provides unique advantages for BC production and morphology profiling by assaying distinct diffraction patterns. With future integration of a sorting component, the target bacteria in the agarose hydrogel particles could be sorted out for downstream gene analysis using polymerase

chain reaction (PCR) technology. The functional sorting of a large-scale mutant library could be achieved in the future to indicate target strains for engineering biology applications. It is worth noting that by conducting a conventional fluorescence labeling approach, BC production within the agarose hydrogel particles could be effectively determined *via* fluorescence intensities. These fluorescence-labeled hydrogel particles could be subjected to standard flow cytometry for particle screening and sorting, while the information correlating to BC morphology would be lost. In addition to addressing the above BC applications, this platform provides a universal approach to rapidly evaluate single-bacterium production amounts and assembly structures using an automatic intelligent platform, which is desirable for a range of applications in biofabrication.

Conflicts of interest

There are no conflicts to declare.

Acknowledgements

We gratefully acknowledge the funding provided by the City University of Hong Kong (9610467), National Research Foundation Singapore, Synthetic Biology Research Program (NRF, SBP), National Research Foundation Singapore, Competitive Research Programme (NRF, CRP), National Medical Research Council Singapore, Open Fund – Individual Research Grant (NMRC, OFIRG) and Ministry of Education (MOE) Singapore, Tier-2.

Notes and references

1 D. Klemm and B. Heublein, *et al.*, Cellulose: fascinating biopolymer and sustainable raw material, *Angew. Chem., Int. Ed.*, 2005, **44**, 3358–3393.
2 A. Sacui and R. C. Nieuwendaal, *et al.*, Comparison of the properties of cellulose nanocrystals and cellulose nanofibrils isolated from bacteria, tunicate, and wood processed using acid, enzymatic, mechanical, and oxidative methods, *ACS Appl. Mater. Interfaces*, 2014, **6**, 6127–6138.
3 P. R. Chawla and I. B. Bajaj, *et al.*, Microbial cellulose: fermentative production and applications, *Food Technol. Biotechnol.*, 2009, **47**, 107–124.
4 U. Romling and M. Y. Galperin, Bacterial cellulose biosynthesis: diversity of operons, subunits, products and functions, *Trends Microbiol.*, 2015, **23**, 545–557.
5 K. T. Powell and J. C. Weaver, Gel Microdroplets and flow cytometry: rapid determination of antibody secretion by individual cells within a cell population, *Bio/Technology*, 1990, **8**, 333.
6 M. Li and M. van Zee, *et al.*, Gelatin microdroplet platform for high-throughput sorting of hyperproducing single-cell-derived microalgal clones, *Small*, 2018, **14**, 1803315.
7 J. Dreier and T. Vollmer, *et al.*, Novel flow cytometry-based screening for bacterial contamination of donor platelet preparations compared with other rapid screening methods, *Clin. Chem.*, 2009, **55**, 1492.
8 A. Alvares-Barrientos and J. Arroyo, *et al.*, Applications of flow cytometry to clinical microbiology, *Clin. Microbiol. Rev.*, 2000, **13**, 167.
9 J. J. Agresti and E. Antipov, *et al.*, Ultrahigh-throughput screening in drop-based microfluidics for directed evolution, *Proc. Natl. Acad. Sci. U. S. A.*, 2010, **107**, 4004–4009.
10 M. Bocchi and M. Lombardini, *et al.*, Dielectrophoretic trapping in microwells for manipulation of single cells and small aggregates of particles, *Biosens. Bioelectron.*, 2009, **24**, 1177–1183.
11 D. K. Wood, D. M. Weingeist, S. N. Bhatia and B. P. Engelward, Single cell trapping and DNA damage analysis using microwell arrays, *Proc. Natl. Acad. Sci. U. S. A.*, 2010, **107**, 10008–10013.
12 S. H. Kim and T. Yamamoto, *et al.*, An electroactive microwell array for trapping and lysing single-bacterial cells, *Biomicrofluidics*, 2011, **5**, 024114.
13 P. Li and X. Q. Dou, *et al.*, Isolated reporter bacteria in supramolecular hydrogel microwell arrays, *Langmuir*, 2017, **33**, 7799.
14 F. R. Devin, *et al.*, Function-driven single-cell genomics uncovers cellulose-degrading bacteria from the rare biosphere, *ISME J.*, 2019, **23**, 1332.
15 A. Basu and S. V. Vadanan, *et al.*, A Novel Platform for Evaluating the Environmental Impacts on Bacterial Cellulose Production, *Sci. Rep.*, 2018, **8**, 5780.
16 E. Brouzes and M. Medkova, *et al.*, Droplet microfluidic technology for single-cell high-throughput screening, *Proc. Natl. Acad. Sci. U. S. A.*, 2009, **106**, 14195–14200.
17 J. C. Baret and O. J. Miller, Fluorescence-activated droplet sorting (FADS): efficient microfluidic cell sorting based on enzymatic activity, *Lab Chip*, 2009, **9**, 1850–1858.
18 H. N. Joensson and H. A. Svahn, Droplet microfluidics-a tool for single-cell analysis, *Angew. Chem., Int. Ed.*, 2012, **51**, 12176–12192.
19 L. Mazutis and J. Gilbert, *et al.*, Single-cell analysis and sorting using droplet-based microfluidics, *Nat. Protoc.*, 2013, **8**, 870–891.
20 T. Konry and M. Dominguez-Villar, *et al.*, Droplet-based microfluidic platforms for single T cell secretion analysis of IL-10 cytokine, *Biosens. Bioelectron.*, 2011, **26**, 2707–2710.
21 E. X. Ng and M. A. Miller, *et al.*, Single cell multiplexed assay for proteolytic activity using droplet microfluidics, *Biosens. Bioelectron.*, 2016, **81**, 408–414.
22 R. Ramji and M. Wang, *et al.*, Single cell kinase signaling assay using pinched flow coupled droplet microfluidics, *Biomicrofluidics*, 2014, **8**, 034104.
23 Y. Yan and D. Boey, *et al.*, Continuous-flow C. elegans fluorescence expression analysis with real-time image processing through microfluidics, *Biosens. Bioelectron.*, 2016, **77**, 428–434.
24 J. R. Choi and H. Song, *et al.*, Microfluidic assay-based optical screening techniques for cell analysis: A review

of recent progress, *Biosens. Bioelectron.*, 2016, **77**, 227–236.

25 J. Q. Yu and T. R. Huang, *et al.*, Production of hollow bacterial cellulose microspheres using microfluidics to form an injectable porous scaffold for wound healing, *Adv. Healthcare Mater.*, 2016, **5**, 2983–2992.

26 J. Q. Yu and W. Huang, *et al.*, Droplet optofluidic imaging for λ-bacteriophage detection via co-culture with host cell Escherichia coli, *Lab Chip*, 2014, **14**, 3519.

27 J. Wang and J. Tavakoli, *et al.*, Bacterial cellulose production, properties and applications with different culture methods – a review, *Carbohydr. Polym.*, 2019, **210**, 63.